Weierstraß–Institut
für Angewandte Analysis und Stochastik

im Forschungsverbund Berlin e.V.

Preprint ISSN 0946 – 8633

Note on weak discontinuity waves in linear poroelastic materials.

Part I: Acoustic waves in saturated porous media.

Krzysztof Wilmański

submitted: 26th March 2002

Weierstrass Institute
for Applied Analysis
and Stochastics
Mohrenstr. 39
D- 10117 Berlin
Germany
E-Mail: wilmansk@wias-berlin.de

Preprint No. 730
Berlin 2002

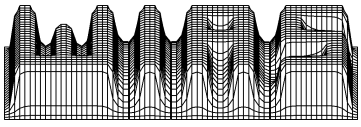

2000 *Mathematics Subject Classification.* 35C20, 35L50, 74J10, 74F10.

Key words and phrases. waves in porous media, monochromatic waves.

Edited by
Weierstraß–Institut für Angewandte Analysis und Stochastik (WIAS)
Mohrenstraße 39
D — 10117 Berlin
Germany

Fax: + 49 30 2044975
E-Mail (X.400): c=de;a=d400-gw;p=WIAS-BERLIN;s=preprint
E-Mail (Internet): preprint@wias-berlin.de
World Wide Web: http://www.wias-berlin.de/

Abstract

The paper contains the analysis of the propagation of acoustic waves in two–component poroelastic media. It is shown that the existence of P2-mode as a wave in the range of low frequencies depends on the way in which the wave is excited. This property as well as properties of other bulk modes are discussed on practical examples of soil mechanics.

1 Introduction

In this work we present three problems of weak discontinuity waves in porous materials: acoustic waves in saturated media modelled by a two–component continuum, surface waves in such media and their asymptotic properties, and acoustic waves in unsaturated porous media modelled by a three–component continuum. The present Part I of the Note is devoted to some aspects of the analysis of dispersion relations for linear poroelastic materials related to the problem of excitation of harmonic acoustic waves in fully saturated systems.

Propagation of acoustic waves in geophysical porous materials plays a particularly important role in testing porous and granular materials because laboratory measurements on such materials usually differ considerably from *in situ* measurements required in practical applications. Most of theoretical results were obtained within the so–called Biot's model (e.g. [1]). They have contributed immensely to the understanding of the subject but simultaneously there are many very controversial issues related to the application of this model. We mention some of them further in this note. During the last decade the acoustics of porous materials was also developed within a different continuous model derived on the basis of a modern continuum thermodynamics. This model in its linear version is on the one hand side simpler than the Biot's model, in contrast to the Biot's model it does not violate the second law of thermodynamics and the principle of material frame indifference, and on the other hand it describes changes of porosity as an additional microscopical variable. In spite of these differences the number of acoustic modes of propagation and their fundamental properties are the same in both models (e.g. [2]).

Part I of the Note contains a review of fundamental properties of P1–, S–, and P2–waves in porous materials. However we emphasize an aspect of such waves which seems to be overlooked in the literature. Namely we demonstrate the dependence of acoustic properties of porous media on the way in which the dynamic disturbance is excited. This way is immaterial for the high frequency asymptotics determining

the speeds of signals in the medium. However it becomes essential in the limit of low frequencies and these are of primary practical importance in soil mechanics and other geophysical applications. We show that the P2–wave does not propagate in the case of impact excitations. This means that some surface modes of propagation[1] cannot appear in the range of low frequencies as well.

2 Field equations for poroelastic media

We consider a two–component poroelastic medium described by the following fields

partial mass density of the fluid $\rho^F(\mathbf{x},t)$,

velocity of the fluid $\mathbf{v}^F(\mathbf{x},t)$,

velocity of the skeleton $\mathbf{v}^S(\mathbf{x},t)$,

symmetric tensor of small deformations of the skeleton $\mathbf{e}^S(\mathbf{x},t)$,

porosity n.

For these fields the following field equations hold in the linear model of poroelastic materials

$$\frac{\partial \rho^F}{\partial t} + \rho_0^F \operatorname{div} \mathbf{v}^F = 0, \tag{1}$$

$$\rho_0^F \frac{\partial \mathbf{v}^F}{\partial t} + \kappa \operatorname{grad} \rho^F + \beta \operatorname{grad}(n - n_0) + \hat{\mathbf{p}} = 0, \quad \hat{\mathbf{p}} := \pi\left(\mathbf{v}^F - \mathbf{v}^S\right), \tag{2}$$

$$\rho_0^S \frac{\partial \mathbf{v}^S}{\partial t} - \operatorname{div}\left(\lambda^S \left(tr\mathbf{e}^S\right)\mathbf{1} + 2\mu \mathbf{e}^S + \beta(n - n_0)\mathbf{1}\right) - \hat{\mathbf{p}} = 0, \tag{3}$$

$$\frac{\partial \mathbf{e}^S}{\partial t} = \operatorname{sym} \operatorname{grad} \mathbf{v}^S, \tag{4}$$

$$\frac{\partial n}{\partial t} + n_0 \operatorname{div}\left(\mathbf{v}^F - \mathbf{v}^S\right) + \frac{n - n_0}{\tau} = 0. \tag{5}$$

In these equations ρ_0^F, ρ_0^S, n_0 denote constant reference values of partial mass densities, and porosity, respectively, and $\kappa, \lambda^S, \mu^S, \beta, \pi, \tau$ are constant material parameters. The first one describes the macroscopic *compressibility* of the fluid component, the next two are macroscopic *elastic constants* of the skeleton, β is the coupling constant, π is the coefficient of *bulk permeability*, and τ is the *relaxation time*. For the purpose of this work we assume $\beta = 0$. Then the problem of evolution of porosity described by equation (5) can be solved separately from the rest of the problem and does not influence the acoustic waves in the medium. Let us mention that the general case has been considered in earlier papers on the subject (e.g. [3],[4]) and it has been shown that coupling effects through β can be neglected in linear models.

[1] see [11] for the high frequency asymptotics

3 Bulk waves

We investigate the propagation of the front carrying weak discontinuities. It is assumed that the front σ_t is given by the relation

$$f(\mathbf{x},t)=0, \quad \mathbf{x}\in\sigma_t\subset\mathcal{B}_t, \quad t\in\mathcal{T}, \tag{6}$$

where the function f is assumed to be at least continuously differentiable with respect to both variables. $\mathcal{B}_t$, $\mathcal{T}$ denote the current configuration of the medium, and the time interval, respectively. The surface defined by (6) moves with the normal speed c and possesses a unit normal vector $\mathbf{n}$ given by the relations

$$c:=-\frac{\frac{\partial f}{\partial t}}{|\operatorname{grad} f|}, \quad \mathbf{n}:=\frac{\operatorname{grad} f}{|\operatorname{grad} f|}. \tag{7}$$

Weak discontinuities of fields introduced in the previous section are defined by the following conditions on the surface σ_t oriented by the field $\mathbf{n}(\mathbf{x},t), \mathbf{x}\in\sigma_t, t\in\mathcal{T}$,

$$\left[\left[\rho^F\right]\right]=0, \quad \left[\left[\mathbf{v}^F\right]\right]=0, \quad \left[\left[\mathbf{v}^S\right]\right]=0, \quad \left[\left[\mathbf{e}^S\right]\right]=0, \tag{8}$$

where

$$[[\ldots]]:=\sigma_t^+\lim(\ldots)-\sigma_t^-\lim(\ldots). \tag{9}$$

Then according to the Hadamard lemma the following kinematic compatibility conditions hold

$$\begin{aligned}\left[\left[\operatorname{grad}\rho^F\right]\right] &= -\frac{1}{c}R^F\mathbf{n}, \quad \left[\left[\operatorname{grad}\mathbf{e}^S\right]\right]=\frac{1}{2c^2}\left(\mathbf{A}^S\otimes\mathbf{n}+\mathbf{n}\otimes\mathbf{A}^S\right)\otimes\mathbf{n}, \\ \left[\left[\operatorname{grad}\mathbf{v}^F\right]\right] &= -\frac{1}{c}\mathbf{A}^F\otimes\mathbf{n}, \quad \left[\left[\operatorname{grad}\mathbf{v}^S\right]\right]=-\frac{1}{c}\mathbf{A}^S\otimes\mathbf{n},\end{aligned} \tag{10}$$

where

$$R^F:=\left[\left[\frac{\partial\rho^F}{\partial t}\right]\right], \quad \mathbf{A}^F:=\left[\left[\frac{\partial\mathbf{v}^F}{\partial t}\right]\right], \quad \mathbf{A}^S:=\left[\left[\frac{\partial\mathbf{v}^S}{\partial t}\right]\right], \tag{11}$$

are the so–called *amplitudes of discontinuity*.

Substitution in field equations evaluated on both sides of the front σ_t yields the conditions

$$R^F=\frac{\rho_0^F}{c}\mathbf{A}^F\cdot\mathbf{n}, \tag{12}$$

and

$$\begin{aligned}\left(c^2\mathbf{1}-\frac{\lambda^S+\mu^S}{\rho_0^S}\mathbf{n}\otimes\mathbf{n}-\frac{\mu^S}{\rho_0^S}\mathbf{1}\right)\mathbf{A}^S &= 0, \\ \left(c^2\mathbf{1}-\kappa\mathbf{n}\otimes\mathbf{n}\right)\mathbf{A}^F &= 0.\end{aligned} \tag{13}$$

Certainly this is the eigenvalue problem which yields three nontrivial solutions:

$$\begin{aligned} c_{P1} &: = \sqrt{\frac{\lambda^S + 2\mu^S}{\rho_0^S}}, \quad \mathbf{A}^S \cdot \mathbf{n} \neq 0, \quad \mathbf{A}^S_\perp := \mathbf{A}^S - \left(\mathbf{A}^S \cdot \mathbf{n}\right)\mathbf{n} = 0, \quad \mathbf{A}^F = 0, \\ c_{P2} &: = \sqrt{\kappa}, \quad \mathbf{A}^F \cdot \mathbf{n} \neq 0, \quad \mathbf{A}^S = 0, \quad \mathbf{A}^F_\perp := \mathbf{A}^F - \left(\mathbf{A}^F \cdot \mathbf{n}\right)\mathbf{n} = 0, \\ c_S &: = \sqrt{\frac{\mu^S}{\rho_0^S}}, \quad \mathbf{A}^S_\perp \neq 0, \quad \mathbf{A}^S \cdot \mathbf{n} = 0, \quad \mathbf{A}^F = 0. \end{aligned} \tag{14}$$

The first two solutions describe longitudinal P1–, and P2–modes of propagation while the third one is the transversal S–mode in the skeleton. There exists no transversal mode in the fluid: $\mathbf{A}^F_\perp \equiv 0$.

The P2–mode is often called Biot's wave. Its theoretical existence is quite natural in the frame of any two–component continuous model even if both components are fluids (a miscible mixture). However there are problems with practical observations of its propagation if one of the components is solid. It has been observed for the first time in an artificial porous material made of sintered glass beads by T. J. Plona [5], and in an artificial rock of cemented sand grains by T. Klimentos and C. McCann [6] but *in situ* measurements are extremally difficult to be performed. The main reason for those difficulties is a very strong attenuation of P2–waves. We discuss this point in some details in this work.

Let us mention in passing that the partial stresses $\mathbf{T}^S, \mathbf{T}^F$ in the skeleton and in the fluid, respectively which lead to the above used field equations are not coupled if the constant β is equal to zero. Such a coupling is required in the Biot's model commonly used in the wave analysis for porous saturated materials. In the notation of this work such a coupling has the form

$$\begin{aligned} \mathbf{T}^S &= \lambda^S \left(tr\mathbf{e}^S\right)\mathbf{1} + 2\mu^S\mathbf{e}^S - Q\frac{\rho^F - \rho_0^F}{\rho_0^F}\mathbf{1}, \\ \mathbf{T}^F &= -\left(\kappa\left(\rho^F - \rho_0^F\right) - Qtr\mathbf{e}^S\right)\mathbf{1}, \end{aligned} \tag{15}$$

where Q is the Biot's coupling constant. Such a model is thermodynamically admissible solely in the case of an additional contribution of the gradient of porosity to the momentum balance equations (2), (3)(see: [7])

$$\hat{\mathbf{p}} = \pi\left(\mathbf{v}^F - \mathbf{v}^S\right) - Q\,\mathrm{grad}\, n. \tag{16}$$

In such a case it can be easily shown that the coefficient Q which would give rise to the off–diagonal terms in the eigenvalue problem (13) has an order of magnitude of the pore pressure, i.e. $10^5\ Pa$ in soils and rocks. This must be compared with elastic constants $\lambda^S, \mu^S, \kappa\rho_0^F$ which are at least of the order $10^8\ Pa$. Hence, similarly to the assumption that $\beta = 0$, we can leave out this correction in the wave analysis.

The above results do not reveal the attenuation of waves because the behaviour of amplitudes cannot be determined from the properties of field equations on the wave front alone. In order to see such effects we have to construct solutions of fields equations. We proceed to do so for monochromatic waves in infinite domains.

4 Monochromatic waves

We seek solutions of the set of equations (1)–(4) in the form of bulk monochromatic waves defined by the following ansatz for harmonic waves

$$\begin{aligned} \rho^F - \rho_0^F &= R^F \mathrm{e}^{i(k\mathbf{n}\cdot\mathbf{x}-\omega t)}, \quad \mathbf{e}^S = \mathbf{E}^S \mathrm{e}^{i(k\mathbf{n}\cdot\mathbf{x}-\omega t)}, \\ \mathbf{v}^F &= \mathbf{V}^F \mathrm{e}^{i(k\mathbf{n}\cdot\mathbf{x}-\omega t)}, \quad \mathbf{v}^S = \mathbf{V}^S \mathrm{e}^{i(k\mathbf{n}\cdot\mathbf{x}-\omega t)}, \end{aligned} \tag{17}$$

where $R^F, \mathbf{E}^S, \mathbf{V}^F, \mathbf{V}^S$ are constant, possibly complex, amplitudes of the disturbance, $\mathbf{n}$ denotes the unit vector in the direction of propagation, k is the wave number, and ω the frequency of the wave. Both k and ω may be complex.

Straightforward calculations lead to the following compatibility relations with field equations

$$R^F = \frac{k\rho_0^F}{\omega}\mathbf{V}^F \cdot \mathbf{n}, \quad \mathbf{E}^S = -\frac{k}{2\omega}\left(\mathbf{V}^S \otimes \mathbf{n} + \mathbf{n} \otimes \mathbf{V}^S\right), \tag{18}$$

$$\begin{aligned} \left(\omega^2\mathbf{1} - \frac{\lambda^S+\mu^S}{\rho_0^S}k^2\mathbf{n}\otimes\mathbf{n} - \frac{\mu^S}{\rho_0^S}k^2\mathbf{1} + i\frac{\pi\omega}{\rho_0^S}\mathbf{1}\right)\mathbf{V}^S - i\frac{\pi\omega}{\rho_0^S}\mathbf{V}^F &= 0, \\ -i\frac{\pi\omega}{\rho_0^F}\mathbf{V}^S + \left(\omega^2\mathbf{1} - \kappa k^2\mathbf{n}\otimes\mathbf{n} + i\frac{\pi\omega}{\rho_0^F}\mathbf{1}\right)\mathbf{V}^F &= 0. \end{aligned} \tag{19}$$

Equations (19) form, of course, the eigenvalue problem with the six–dimensional eigenvector $\left(\mathbf{V}^S, \mathbf{V}^F\right)^T$, and ω^2 – eigenvalues if k is given. We consider further also a modification of this problem with a given ω.

We can easily separate the components in the direction of the vector $\mathbf{n}$, and in the direction perpendicular to this vector. We consider these problems in the subsequent two sections.

5 Longitudinal modes of propagation

Scalar multiplication of equations (19) by the vector $\mathbf{n}$ yields

$$\begin{pmatrix} \omega^2 - \lambda^S + 2\mu^S\rho_0^S k^2 + i\pi\omega\rho_0^S & -i\pi\omega\rho_0^S \\ -i\pi\omega\rho_0^F & \omega^2 - \kappa k^2 + i\pi\omega\rho_0^F \end{pmatrix} \begin{pmatrix} \mathbf{V}^S \cdot \mathbf{n} \\ \mathbf{V}^F \cdot \mathbf{n} \end{pmatrix} = 0. \tag{20}$$

This two–dimensional eigenvalue problem yields immediately the following *dispersion relation*

$$\left(\omega^2 - c_{P1}k^2 + i\pi\omega\rho_0^S\right)\left(\omega^2 - c_{P2}^2k^2 + i\pi\omega\rho_0^F\right) + \frac{\pi^2\omega^2}{\rho_0^S\rho_0^F} = 0. \tag{21}$$

We consider two cases.

1. The frequency ω is real and given. This corresponds to the problem of a harmonic excitation with a given frequency ("boundary value problem").

2. The wave number k is real and given. This corresponds to an external impact ("initial value problem").

In the first case the equation (21) can be easily solved for k and we obtain

$$k^2 = \frac{1}{2}\left[\frac{1}{c_{P1}^2}\left(\omega^2 + i\frac{\pi\omega}{\rho_0^S}\right) + \frac{1}{c_{P2}^2}\left(\omega^2 + i\frac{\pi\omega}{\rho_0^F}\right) \pm \sqrt{D}\right], \tag{22}$$

$$D := \left[\frac{1}{c_{P1}^2}\left(\omega^2 + i\frac{\pi\omega}{\rho_0^S}\right) - \frac{1}{c_{P2}^2}\left(\omega^2 + i\frac{\pi\omega}{\rho_0^F}\right)\right]^2 - \frac{4}{c_{P1}^2 c_{P2}^2}\frac{\pi^2\omega^2}{\rho_0^S\,\rho_0^F}.$$

In the next two Figures we illustrate this result for the following numerical data

$$\begin{aligned} c_{P1} &= 2500\frac{m}{s}, \quad c_{P2} = 1000\frac{m}{s}, \\ \rho_0^S &= 2500\frac{kg}{m^3}, \quad \rho_0^F = 250\frac{kg}{m^3}. \end{aligned} \tag{23}$$

In Figure 1 we plot the phase velocity $c_{ph} = \omega Re k$of both longitudinal modes, and in the Figure 2 the attenuation $\gamma = Imk$.

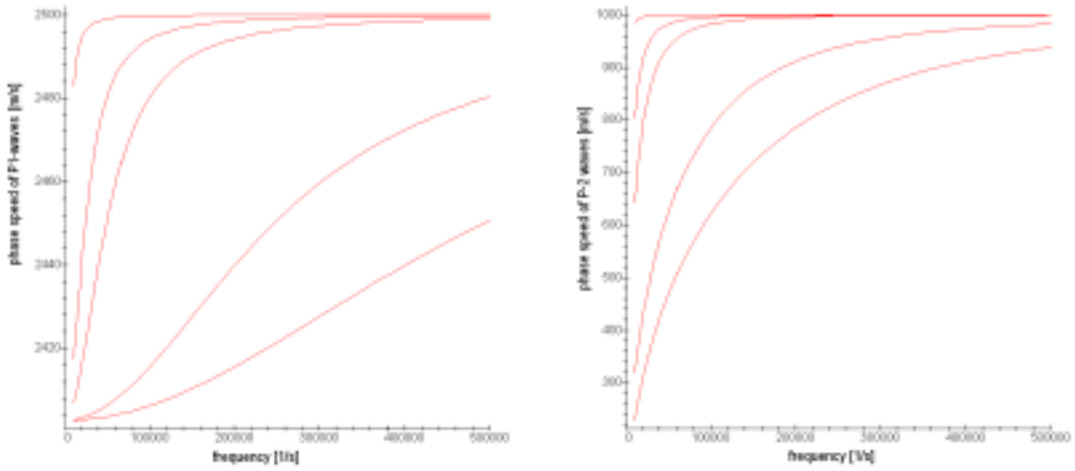

Figure 1: *Phase speed of P1– (left), and P2–waves (right) as functions of frequency ω.*

The curves correspond to the permeability π (from top to bottom): $10^6, 5*10^6, 10^7, 5*10^7, 10^8$ $[\frac{kg}{m^3 s}]$.

Inspection of the Figure 1 shows that both modes of propagation exist for any frequency of the excitation. The phase speed of P1–waves grows a little from its initial value to the asymptotic speed c_{P1} for $\omega \to \infty$. On the other hand the phase speed of P2–waves is equal to zero for $\omega = 0$ and grows asymptotically to the limit c_{P2} for $\omega \to \infty$. For both modes the growth becomes slower for larger permeability coefficients π.

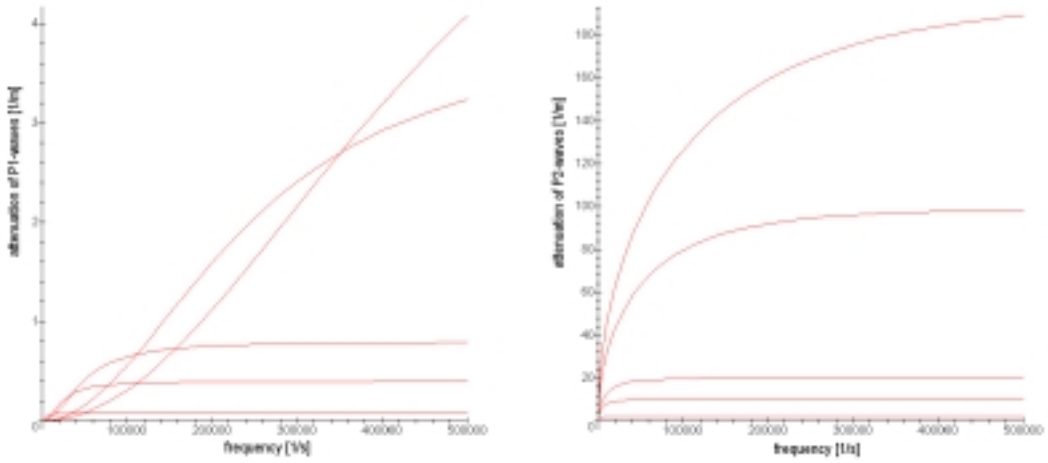

Figure 2: *Attenuation of P1– (left), and P2–waves (right) as functions of frequency ω.*

The same values of permeability π as in Fig.1 growing from the bottom to the top.

It is clear from Figure 2 that the attenuation of P2–waves is much stronger than this of P1–waves. This observation justifies the remark made in the Introduction that the strong attenuation of P2–waves causes difficulties in their *in situ* measurements.

The above described properties of monochromatic waves have been discussed in details in earlier works on this model of poroelastic materials (e.g. [8], [9], [4], [3], [10]).

We proceed to present properties of the second case – external impact (initial value problem). In this case the wave number k is given and real, and the frequency ω is complex. It follows as the solution of the dispertion relation (21). This solution cannot be obtained analytically and we present here a few typical numerical examples. We use the data (23).

In contrast to the above discussed boundary value problem P2–waves may not exist in the case of the initial value problem. For any chosen real wave number k solutions of the dispersion relation (21) consists of four complex ω symmetric with respect to zero. Consequently there are two essential real parts of ω which determine P1–, and P2–mode. In Figure 3 we show the real part of ω corresponding to the P2–mode for

different values of the permeability coefficient π. It is seen that that for sufficiently low wave numbers k (i.e. long waves) the real part of ω is constant and equal to zero. Consequently in these ranges the P2–modes contain only damping and they cannot propagate as waves. The extent of the plateau of the constant real part of frequency changes approximately in the linear way with π and, for instance, for $\pi = 10^9[\frac{kg}{m^3 s}]$ (the right figure) it reaches the value $k \approx 2050[\frac{1}{m}]$, which corresponds to the wave length $0.05cm$. Obviously from the physical point of view P2–wave does not exist any more because the wave length would have to be smaller than the characteristic dimension of the microstructure. However the minimum length of the wave for smaller permeabilities lie in the physically reasonable range. For instance for $\pi = 10^7[\frac{kg}{m^3 s}]$ it is app. $5cm$ (see the left figure).

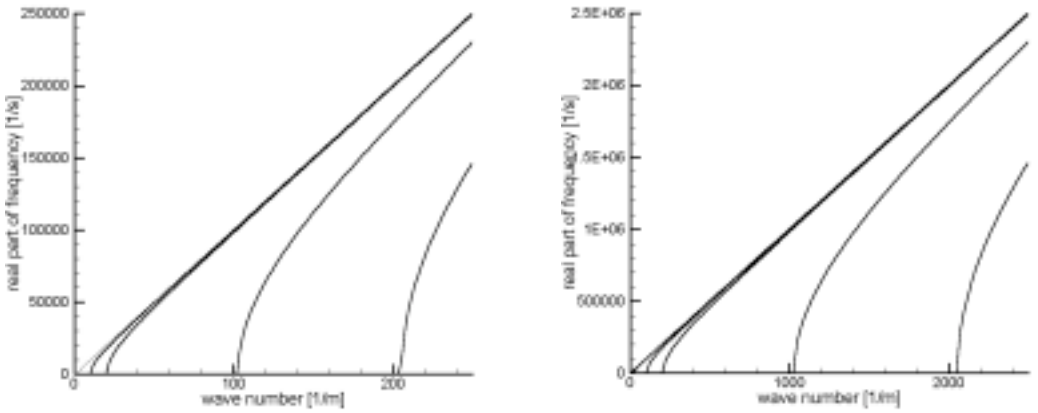

Figure 3: *Real part of the frequency as a function of the wave number for P2–waves.*

The left hand side is the magnification of the figure on the right hand side for the following values of permeability π: $10^6, 5*10^6, 10^7, 5*10^7, 10^8$ $[\frac{kg}{m^3 s}]$ growing from the left to the right. On the right figure the curves for $\pi = 5*10^8$ and 10^9 $[\frac{kg}{m^3 s}]$ are shown in addition.

The problem of existence of propagation does not concern the P1–mode. These waves behave in a way similar to these of the boundary value problem. In Figure 4 we show their phase speeds for the data (23). The speed grows a little and reaches the limit value c_{P1} for $k \to \infty$.

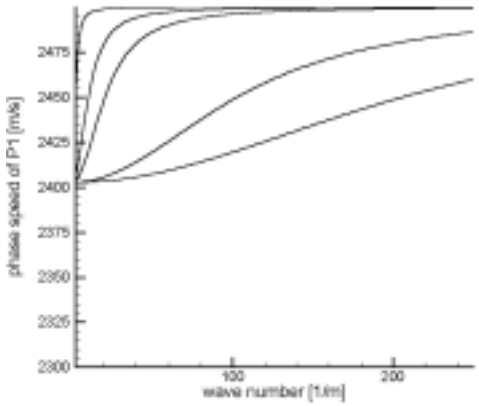

Figure 4: *Phase velocity of P1–waves for permeability π (from the left to the right)*: $10^6, 5*10^6, 10^7, 5*10^7, 10^8$ $[\frac{kg}{m^3 s}]$

As indicated above the P2–waves do not propagate below a critical value of k which changes with π. We show this behaviour in Figure 5. In the range of large values of k the P2–modes propagate and reach the limit value c_{P2} for $k \to \infty$.

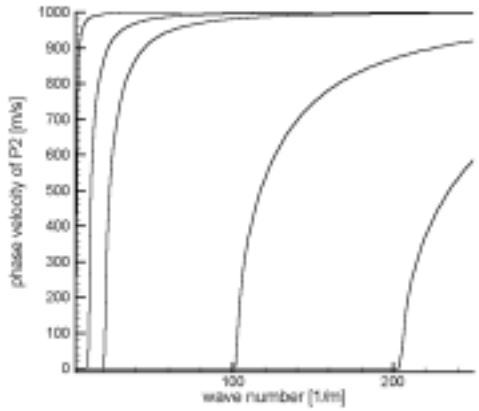

Figure 5: *Phase velocity of P2–waves for permeability π (from the left to the right)*: $10^6, 5*10^6, 10^7, 5*10^7, 10^8$ $[\frac{kg}{m^3 s}]$

Imaginary parts of the frequency ω determine the damping of waves. This attenuation in time behave differently from the attenuation in space discussed in the first case. In the case of P1–waves (Figure 6) it grows with the growth of the wave number k (i.e. with the decay of the wave length). However in the range of long waves the damping in media with a larger permeability π is smaller than this for media with a smaller permeability. Most likely it is related to the fact that the energy of

the wave created by the impact remains longer in the vicinity of the impact if the value of π is larger which, as seen in Figure 4 yields a lower speed of propagation.

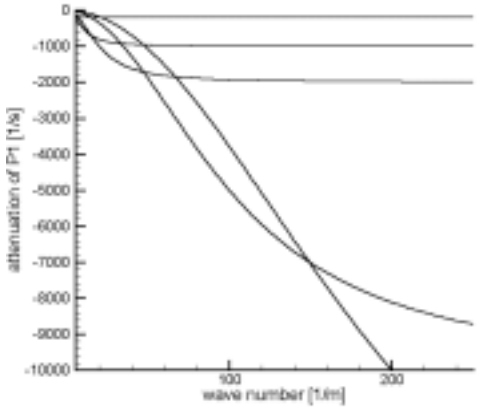

Figure 6: *Attenuation of P1–waves for permeability* π: 10^6 *(the smallest attenuation),* $5 * 10^6, 10^7, 5 * 10^7, 10^8$ *(the largest attenuation)* $[\frac{kg}{m^3 s}]$.

The behaviour of P2–modes is entirely different due to the existence of plateau. The ranges of these plateaus are visible also in Figure 7 which illustrates the attenuation of P2–modes. For any value of permeability π the range of small values of k contains solely the damping – the frequency ω is imaginary. For larger values of k we see the attenuation of P2–waves. As in the case of the boundary value problem it is much stronger than in the case of P1–waves.

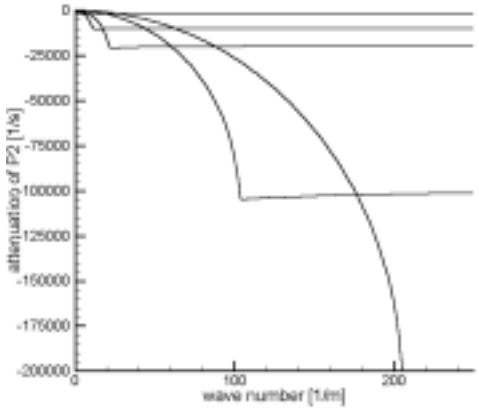

Figure 7: *Attenuation of P2–waves for permeability* π: 10^6 *(the smallest attenuation),* $5 * 10^6, 10^7, 5 * 10^7, 10^8$ *(the largest attenuation)* $[\frac{kg}{m^3 s}]$

The above described properties of initial value problems have an important influence on the construction of asymptotic solutions in the range of low frequencies. For

instance, they lead to an entirely different structure of surface waves than this for high frequencies [11]. We shall discuss this problem in the Part II of this Note.

6 Transversal modes of propagation

Let us introduce the following quantities

$$\mathbf{V}^F_\perp := \mathbf{V}^F - \left(\mathbf{V}^F \cdot \mathbf{n}\right) \mathbf{V}^F, \quad \mathbf{V}^S_\perp := \mathbf{V}^S - \left(\mathbf{V}^S \cdot \mathbf{n}\right) \mathbf{V}^S. \tag{24}$$

Then from (19) for arbitrary components of the above vectors $V^F_\perp := \mathbf{V}^F_\perp \cdot \mathbf{t}$, $V^S_\perp := \mathbf{V}^S_\perp \cdot \mathbf{t}$, with $\mathbf{t}$ being any unit vector perpendicular to $\mathbf{n}$ we obtain

$$\begin{pmatrix} \omega^2 - \mu^S \rho^S_0 k^2 + i\pi\omega\rho^S_0 & -i\pi\omega\rho^S_0 \\ -i\pi\omega\rho^F_0 & \omega^2 + i\pi\omega\rho^F_0 \end{pmatrix} \begin{pmatrix} V^S_\perp \\ V^F_\perp \end{pmatrix} = 0. \tag{25}$$

This is again the eigenvalue problem which yields the dispertion relation

$$\omega^3 + i\pi \left(1\rho^S_0 + 1\rho^F_0\right) \omega^2 - c^2_S k^2 \omega - i c^2_S k^2 \pi \rho^F_0 = 0. \tag{26}$$

We illustrate the solutions of this relation in Figures 8 and 9 for the data

$$\begin{aligned} c_S &= 1500 \frac{m}{s}, \\ \rho^S_0 &= 2500 \frac{kg}{m^3}, \quad \rho^F_0 = 250 \frac{kg}{m^3}. \end{aligned} \tag{27}$$

We obtain for the phase speed the behaviour quite similar to this of P1–waves. After the initial growth the phase speed goes to the limit value c_S for $k \to \infty$.

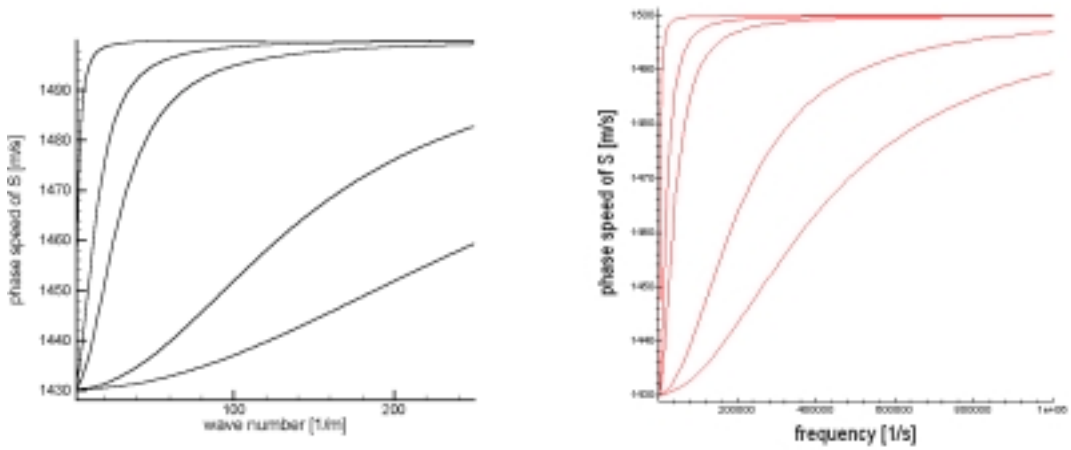

Figure 8: *Phase speed of S–waves for the permeability* π : $10^6, 5 * 10^6, 10^7, 5 * 10^7, 10^8$ $[\frac{kg}{m^3 s}]$.

The left diagrams correspond to the initial value problem while the right diagrams to the impact.

The upper curve corresponds to the lowest permeability.

The behaviour of the attenuation is also similar to this of P1–waves. The rate of attenuation is similar as well as the comparison of the values of $Im\omega$ for both waves cleary shows.

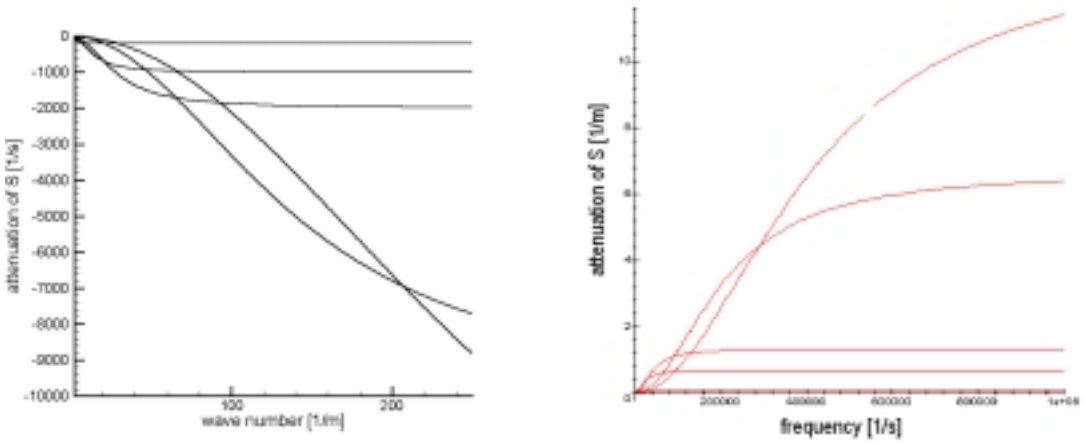

Figure 9: *Attenuation of S–waves for the permeabilities* π:

$10^6, 5 * 10^6, 10^7, 5 * 10^7, 10^8$ $[\frac{kg}{m^3 s}]$.

The left diagrams correspond to the initial value problem while the right diagrams to the impact.

The upper curve corresponds to the lowest permeability.

7 Final remarks

Results presented in this work show that the simplest possible model of saturated poroelastic materials yields qualitatively the same properties of wave motion as more sofisticated Biot's model. However in contrast to the latter the model used in this paper does not contradict any principal rules of the modern continuum thermodynamics. In addition the notions such as tortuosity, anisotropic permeability, etc. which may be essential in some practical applications are not needed in the construction of all important bulk modes of propagation in spite of claims in the literature on the Biot's model.

As the analysis of monochromatic waves shows the asymptotic behaviour for high frequencies checks with the expectation following from the analysis of singularities

of fields independently of the fact if one controls the propagation by harmonic excitations on the boundary (a given real frequency ω) or if one controls an initial condition in which a wave of a particular length (a given real wave number k) is excited.

However the situation changes if we consider a low frequency limit. This limit is smooth independently of the external control for the classical two modes of propagation – P1–waves and S–waves. Both these waves have finite phase speeds for $\omega \to 0$ and these are a bit smaller than the speeds of propagation of the corresponding fronts. This is not the case for the P2-mode. This mode behave like a wave for harmonic excitations on the boundary. The phase speed of this wave goes to zero as $\omega \to 0$. In the vicinity of the zero frequency it has approximately a parabolic character. The behaviour changes entirely in the case of initial conditions. In the vicinity of the zero point of the wave number k (infinitely long waves) the P2–mode has the zero phase velocity and it is solely damped. After a plateau of the zero velocity whose length depends on the value of the permeability coefficient π this mode behaves again as a wave and in the limit of high frequencies (short waves) this behaviour is the same as this of the P2–waves excited by harmonic vibrations.

Such a behaviour has a very important practical bearing. First of all the lack of positive results for the P2–waves in *in situ* measurements may be related not only to the high attenuation of P2-waves but also to the nonexistence of these waves for low frequency initial excitations. It is also very important in the analysis of surface waves in the range of low frequencies commonly used in geophysical applications. We will return to this question in the Part II of this Note.

Let us mention finally that the attenuation properties of all modes are caused by the relative motion of components reflected by the permeability coefficient π. As the examples presented in the paper clearly show these properties check well with the expectations.

References

[1] T. Bourbie, O. Coussy, B. Zinszner; *Acoustics of porous media*, Editions Technip, Paris (1987).

[2] K. Wilmanski; On weak discontinuity waves in porous materials, in: *Trends in applications of mathematics to mechanics*, M. Marques, J. Rodrigues (eds.), 71-83, Longman, N.Y. (1995).

[3] K. Wilmanski; Thermodynamics of Multicomponent Continua, in: *Earthquake Thermodynamics and Phase Transformations in the Earth's Interior*, R. Teisseyre, E. Majewski (eds.), Chapt. 25, 567-671, Academic Press, San Diego (2001).

[4] K. Wilmanski; Waves in Porous and Granular Materials, in: *Kinetic and Continuum Theories of Granular and Porous Media*, K. Hutter, K. Wilmanski

(eds.), 131-186, CISM Courses and Lectures No. 400, Springer Wien New York (1999).

[5] T. J. Plona; Observation of a second bulk compressional wave in a porous medium at ultrasonic frequencies: *Appl. Phys. Lett.*, **36**, 259–261 (1980).

[6] T. Klimentos, C. McCann; Why is the Biot slow compressional wave not observed in real rocks? *Geophysics*, **53**, 12, 1605–1609 (1988).

[7] R. Lancellota, K. Wilmanski; Biot's model and nondestructive testing of granular materials by means od acoustic measurements, WIAS–Preprint (in preparation, 2002).

[8] K. Wilmanski; Dynamics of Porous Materials under Large Deformations and Changing Porosity, in: *Contemporary Research in the Mechanics and Mathematics of Materials*, R. C. Batra, M. F. Beatty (eds.), 343-358 (1996).

[9] K. Wilmanski; *Thermomechanics of Continua*, Springer, Berlin (1998).

[10] K. Wilmanski; Sound and shock waves in porous and granular materials: in: *Proceedings "WASCOM 99", 10th Conference on Waves and Stability in Continuous Media*, V. Ciancio, A. Donato, F. Oliveri, S. Rionero (eds.), 489-503 (2001).

[11] I. Edelman, K. Wilmanski; Asymptotic analysis of surface waves at vacuum/porous medium and liquid/porous medium interfaces, *Cont. Mech. Thermodyn.*, **14**, 1, 25-44 (2002).